Supporting information

Kinetically stable lanthanide complexes displaying exceptionally high quantum yields upon long wavelength excitation: Synthesis, photophysical properties and solution speciation

*Jack D. Routledge, Michael W. Jones, Stephen Faulkner and Manuel Tropiano**

University of Oxford, Chemistry Research Laboratory, 12 Mansfield Road, Oxford OX1 3TA, UK.

Table of Contents

General procedures 2
Synthesis and characterisations 2
Details of photophysical studies 2
Synthetic procedures 3
Synthesis of S3 3
Synthesis of S5 3
HPLC 3
HPLC profiles of Eu(III) complexes 4
High resolution mass spectra of lanthanide complexes 5
NMR spectra 7
NMR spectra of $Lu.L^1$ and $[Lu.L^1]^-$ 7
NMR spectra of $Eu.L^2$ 9
NMR spectra of $Eu.L^3$ and $[Eu.L^3]^-$ 10
NMR spectra of $Yb.L^2$ 11
NMR spectra of $Yb.L^3$ and $[Yb.L^3]^-$ 12
Emission and UV-vis spectra 13
Comparison of emission spectra of $Eu.L^1$ at start and end of pH titration 13
pH dependent UV-Vis absorption and emission spectra of Ln(III) compounds 14
Lifetime emission decay curves of lanthanide complexes 17
X-ray Crystallography 23
References 25

General procedures

Synthesis and characterisations

Commercially available solvents and chemicals were used without further purification unless otherwise stated. Cyclen was purchased from Chematech, lanthanide salts were purchased from Strem Chemicals while solvents were purchased from Sigma Aldrich. NMR spectra were recorded on a Bruker AVIII 400 or AVIII 500 spectrometer as specified. All chemical shift (δ) values are given in parts per million. Low-resolution mass spectra were recorded on a Waters Micromass LCT Premier XE spectrometer. Accurate masses were determined to four decimal places using Bruker µTOF and Micromass GCT spectrometers at the Chemistry Research Laboratory of the University of Oxford. A Hannah pH meter was used for pH measurements of solution of complexes in water and deuterium oxide. In the case of deuterium oxide (particularly for NMR studies), the value reported here is the pH value given by the instrument with pD = pH + 0.45 as reported in the literature.[1]

Details of photophysical studies

UV-visible spectroscopy was performed using a PG instruments T60 UV/VIS spectrophotometer. All emission spectra were recorded at room temperature and in steady state mode unless otherwise stated. Luminescence spectra were measured on a Horiba Jobin Yvon FluoroLog-3 equipped with a Hamamatsu R928 detector and a double-grating emission monochromator. Emission lifetimes were obtained on the same system equipped with a Xenon flash lamp. Luminescence lifetimes were obtained by tail fit for Eu(III) complexes, using a spreadsheet running in Microsoft Excel or using the Fluoressence™ software. All lifetimes gave satisfactory fitting using a mono exponential decay function; fitting to a double exponential decay did not improve the fit unless otherwise stated. Quantum yield for Eu(III) complexes were recorded relative to cresyl violet in methanol and the compound reported by Bünzli *et al.* using the conditions therein reported.[2] Where quantum yields and molar absorption coefficient were measured (in the case of Eu(III) compounds), the complexes were further purified by semipreparative HPLC. Studies of the pH dependence of the photophysical properties of lanthanide compounds were carried out using a Hannah pH meter using 0.1 M NaOH or HCl for pH adjustments; in every case dilution at the end of the titration was less than 5% of the initial volume. Near-infrared luminescence spectra from Yb(III) complexes were measured on the same Horiba Jobin Yvon FluoroLog-3 system equipped with a Hamamatsu R5509-42 NIR PMT InGaAs detector cooled to -80° C. In the case of lifetimes luminescence measurements of Yb(III) complexes, the sample was excited using a pulsed nitrogen laser (PTI-3301-337nm). Light emitted at right angles to the excitation beam was focused onto the slits of the monochromator (PTI120), which was used to select the appropriate wavelength (980 nm). The growth and decay of the luminescence at selected wavelengths was detected using a germanium photodiode (Edinburgh Instruments, EI-P) and recorded using a digital oscilloscope (Tektronix TDS220) before being transferred to the computer for analysis. Luminescence lifetimes were obtained by iterative deconvolution of the detector response (obtained by using a scatter) with exponential components for growth and decay of the metal centred luminescence. Triplet state emission spectra at 77 K were measured on a Perkin Elmer LS55 spectrophotometer equipped with an Oxford Instrument cryostat on samples prepared in ethanol.

Synthetic procedures

Synthesis of S3

S3 was synthesised according to a literature procedure.[3] The product was obtained as a white powder upon purification by silica gel column chromatography (Hexane with up to 10% EtOAc). Crystals were formed upon slow evaporation of a hexane:ethyl acetate solution. ^{1}H NMR (400 MHz; $CDCl_3$): δ 8.75 (s, 1H), 8.17 (d, J = 8.0 Hz, 1H), 8.12 (d, J = 8.0 Hz, 1H), 7.55 (t, J = 8.0 Hz, 1H), 7.46 (t, J = 8.0 Hz, 2H), 7.34 (t, J = 8.0 Hz, 1H), 4.85 (s, 2H), 4.41 (q, J = 8.0 Hz, 2H), 1.48 (t, J = 8.0 Hz, 3H). LR-ESMS: *m/z* calc. for $[M+H]^+$ 272.1, found 272.1.

Synthesis of S5

3-Acetylphenanthrene (0.41 g, 1.86 mmol) was dissolved in diethyl ether (10 ml) and dioxane (5 ml) and the mixture stirred in an ice bath while Br_2 was added dropwise (0.1 ml, 1.86 mmol). The reaction was left stirring at RT monitoring its progression by TLC. After typically 3 hours all starting material was consumed. Water (30 ml) was added to the organic mixture and the aqueous layer was extracted with diethyl ether (3 x 30 ml). The organic solvent was dried with brine, $MgSO_4$ and evaporated. The crude product was purified by silica gel chromatography (1:1 (v:v) DCM:light petroleum ether) to obtain a yellow oil (0.313 g, 56%). ^{1}H-NMR (400 MHz; $CDCl_3$): δ 9.33 (s, 1H), 8.74 (d, J = 8.0 Hz, 1H), 8.11 (d, J = 8.0 Hz, 1H), 7.92 (m, 2H), 7.86 (d, J = 8.0 Hz, 1H), 7.73 (m, 2H), 7.66 (t, J = 8.0 Hz, 1H), 4.62 (s, 2H). ^{13}C NMR (101 MHz; $CDCl_3$): δ 191.4, 135.5, 132.2, 131.5, 130.5, 130.3, 129.9, 129.1, 128.9, 127.5, 127.4, 126.2, 125.6, 124.8, 122.7, 31.1. LR-ESMS: m/z calc. for $[M+Na]^+$ 322.2, found 323.0.

HPLC

HPLC traces were measured using a Gilson analytical HPLC equipped with a Gilson 322 dual pump and a Gilson 152 UV-Vis detector. The stationary phase used was a Discovery Cyano analytical HPLC column and the gradient conditions used are described in the table below:

Time	**Acetonitrile (0.1% formic acid)**	**Water (0.1% formic acid)**	**Flow rate (ml/min)**
0-3	5	95	1
15-20	95	5	1
22-25	5	95	1

HPLC profiles of Eu(III) complexes

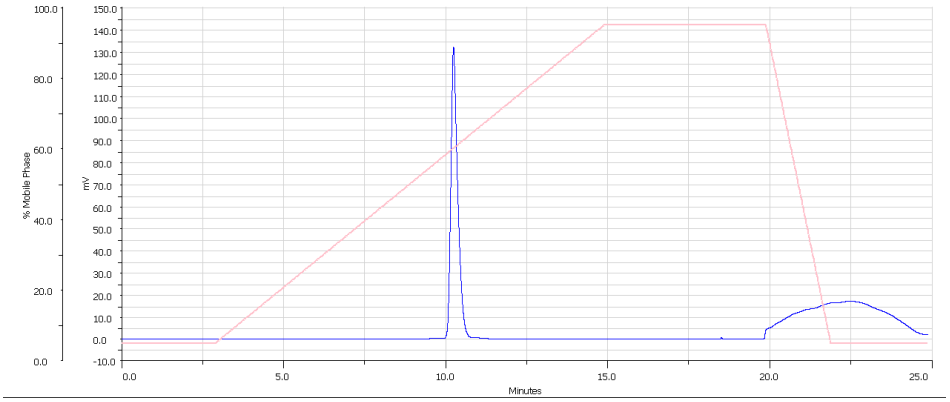

Figure S 1.HPLC profile of **Eu.L**[1], λ = 350 nm. Slow bubble discharge from detector cell between 20-25 minutes.

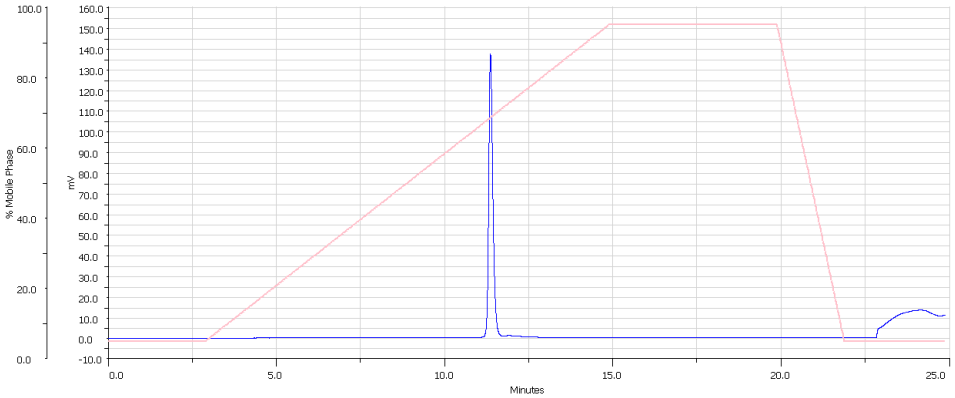

Figure S 2. HPLC profile of **Eu.L**[2], λ = 360 nm. Slow bubble discharge from detector cell between 23-25 minutes.

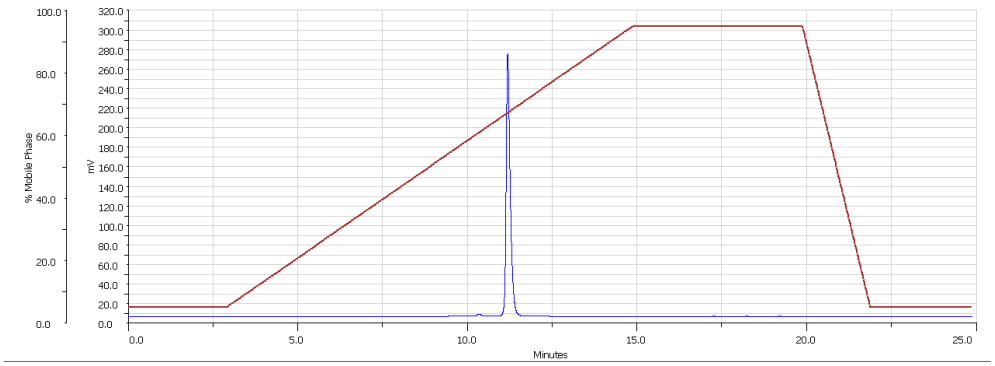

Figure S 3. HPLC profile of **Eu.L**[3], λ = 350 nm.

High resolution mass spectra of lanthanide complexes

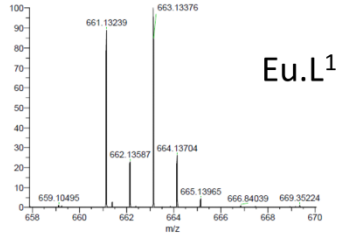

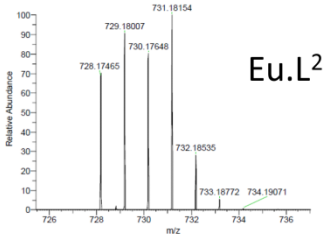

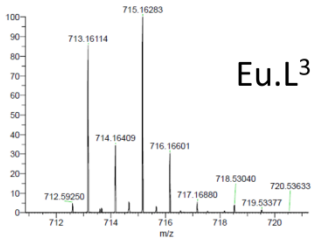

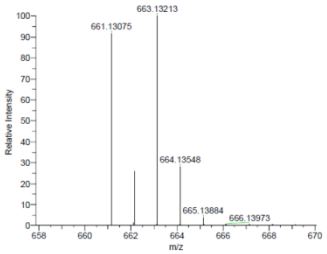

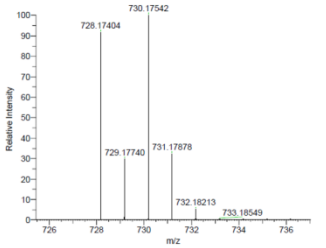

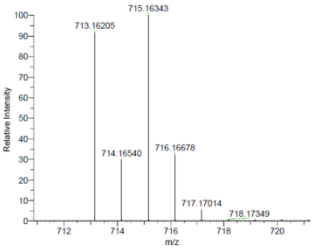

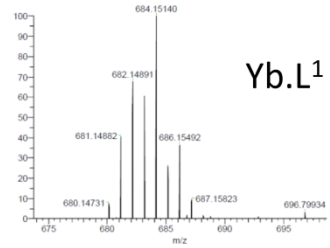

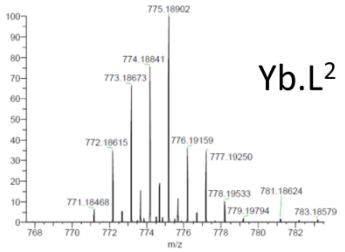

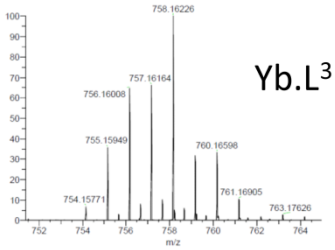

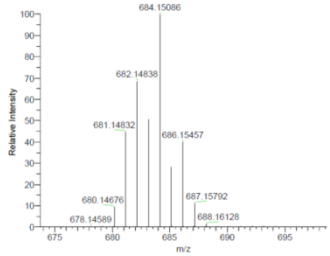

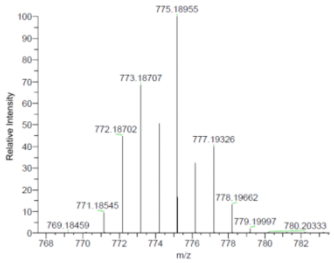

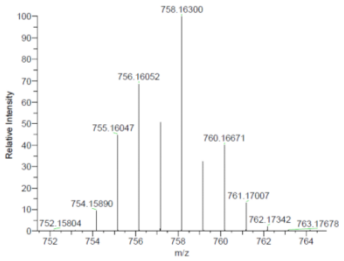

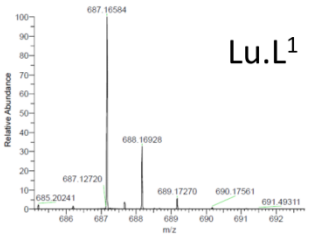

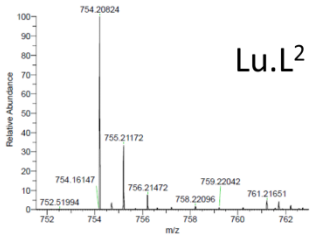

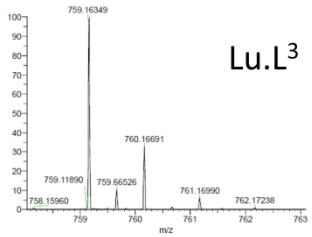

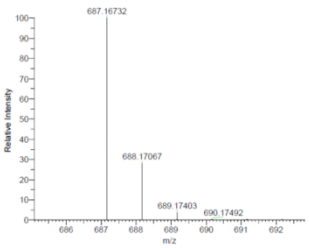

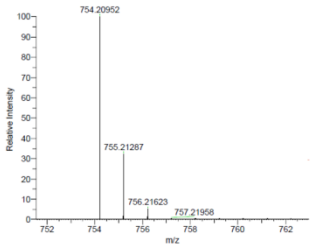

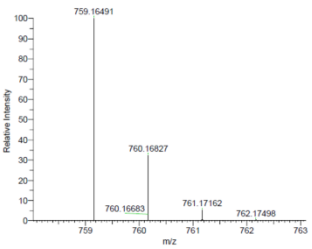

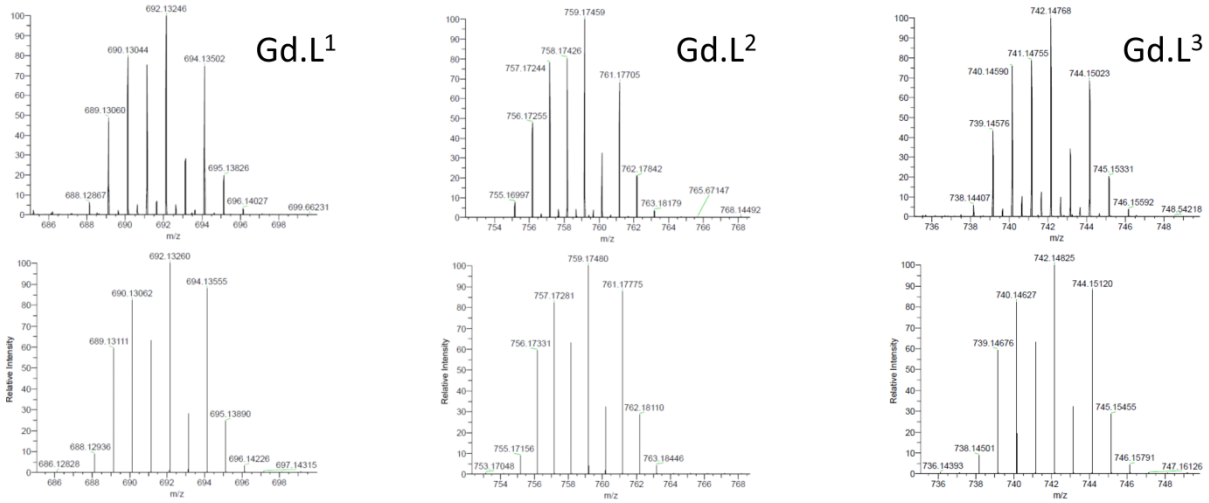

Figure S 4. High resolution mass spectra of the lanthanide complexes prepared in this work reporting the measured spectrum (top) and the theoretical spectrum (bottom).

NMR spectra

NMR spectra of Lu.L^1 and [Lu.L^1]$^-$

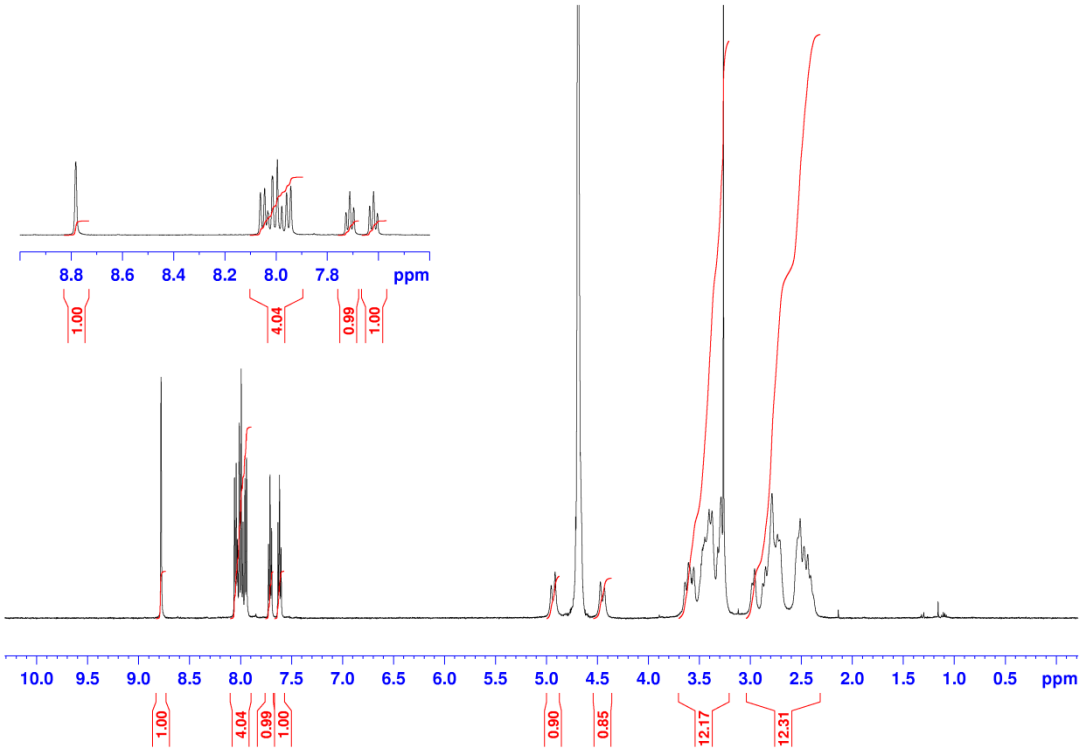

Figure S 5. ^{1}H-NMR of a fresh sample of **Lu.L^1** at pH 5 in D_2O (T = 298 K) measured 5 minutes after sample preparation. The inset shows a zoom into the 7.7 to 9.0 ppm region.

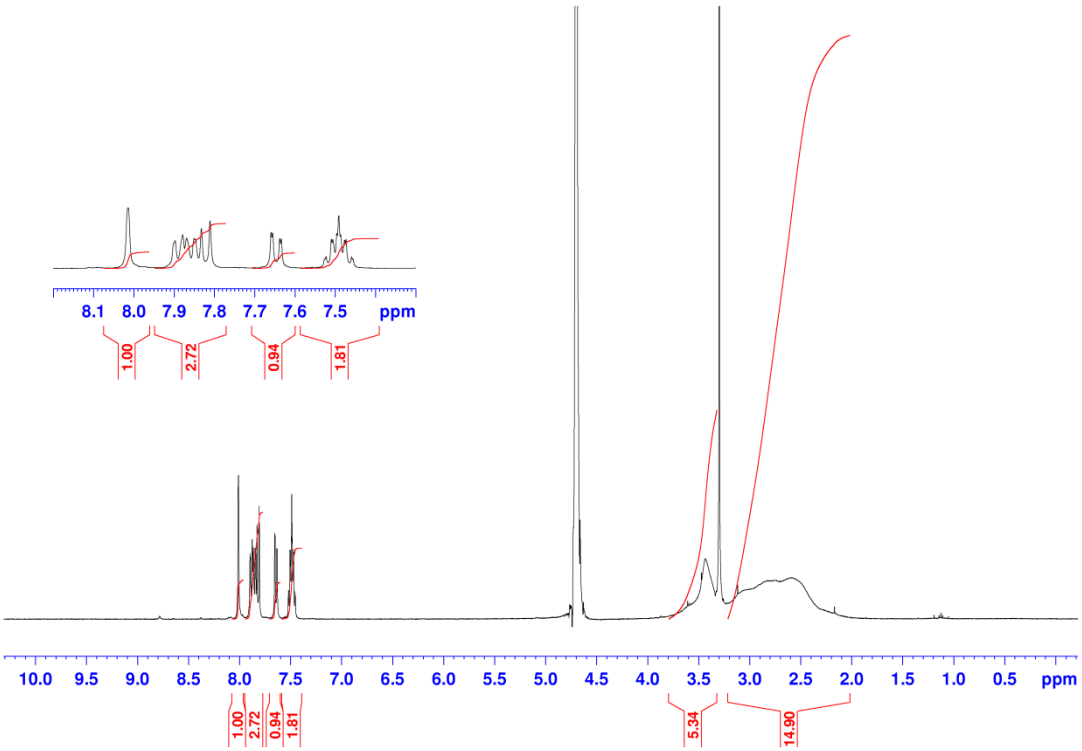

Figure S 6. ^{1}H-NMR of a fresh sample of **[Lu.L^{1}]$^{-}$** at pH 12 in D_2O (T = 298 K). The inset shows a zoom into the 7.0 to 8.5 ppm region.

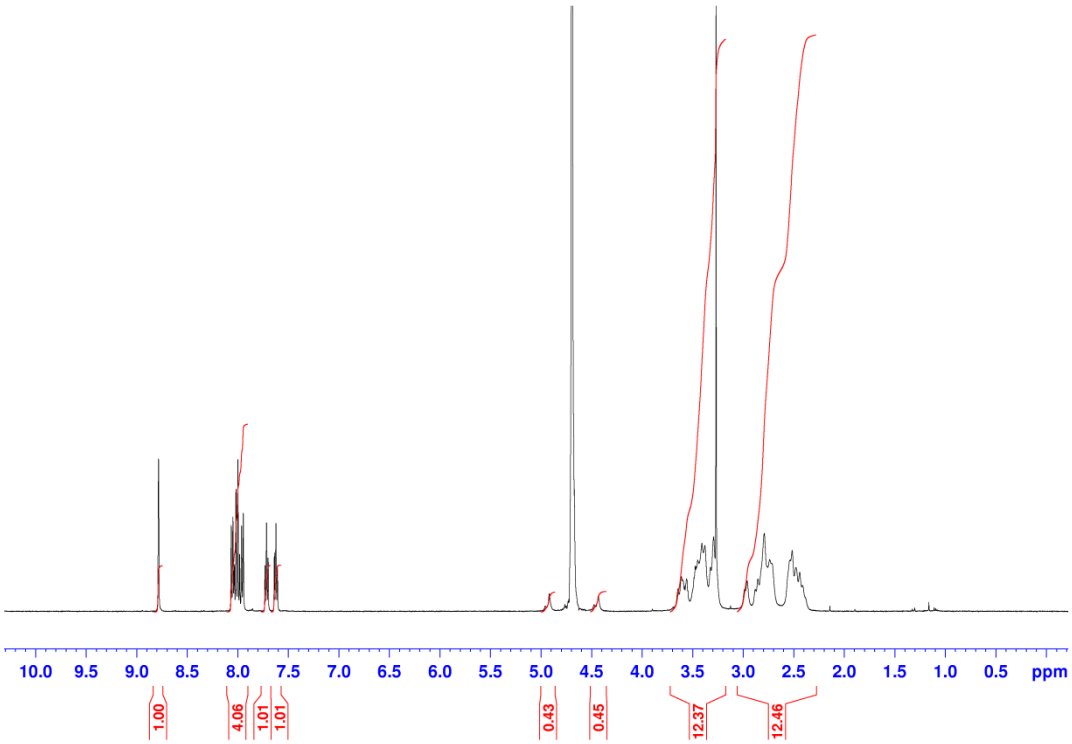

Figure S 7. Lu.L^{1} at pH 5 (D_2O, T = 298 K) after 16 hours equilibration time, showing the decrease in the integral value of the CH_2 protons in alpha to the ketone carbonyl due to exchange with deuterium.

NMR spectra of Eu.L^2

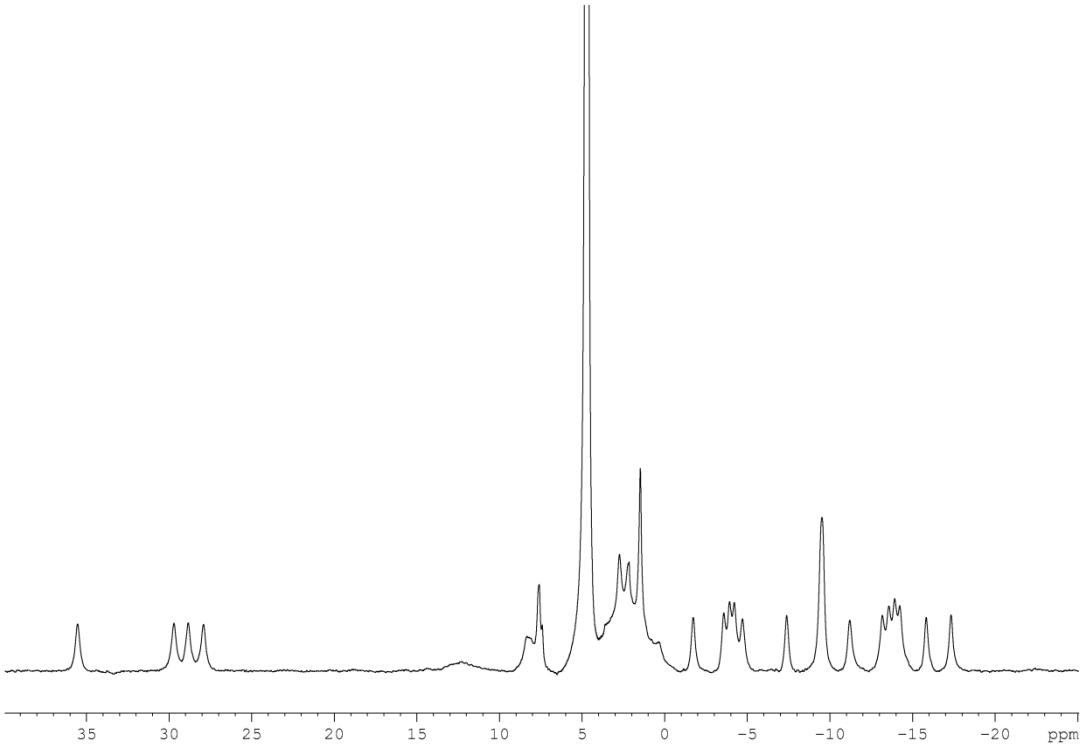

Figure S 8. ^{1}H-NMR of **Eu.L^2** in D_2O, pH 7, T = 298K.

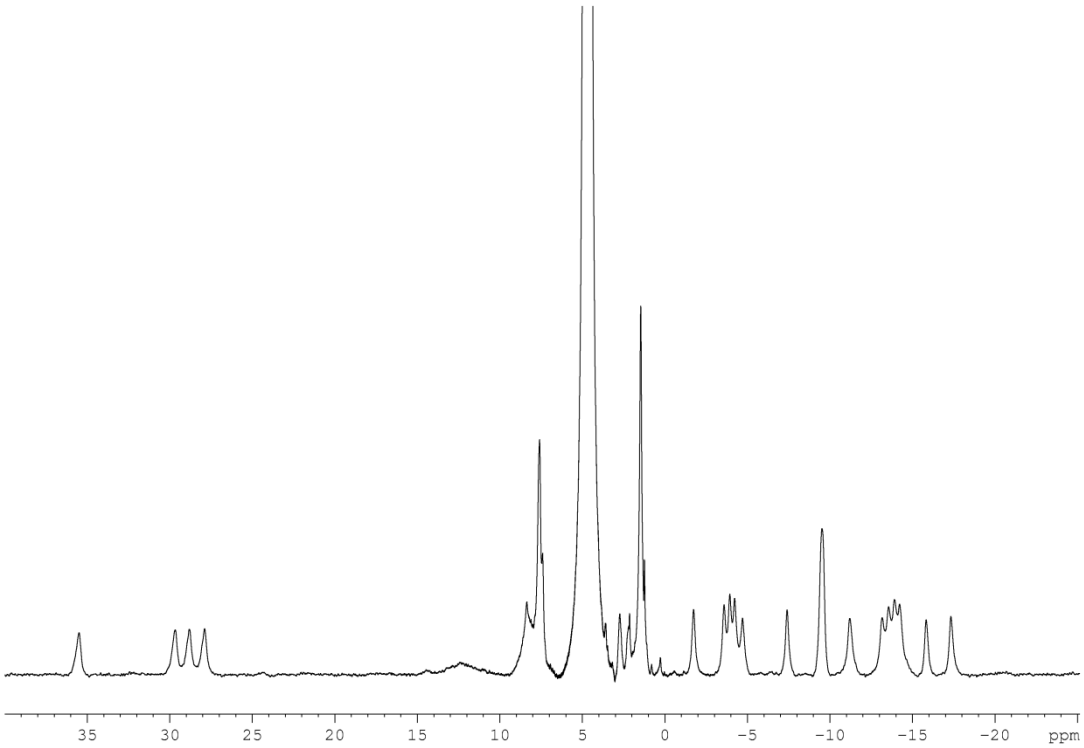

Figure S 9. ^{1}H-NMR of **Eu.L^2** in D_2O, pH 12, T = 298K.

NMR spectra of Eu.L^3 and [Eu.L^3]$^-$

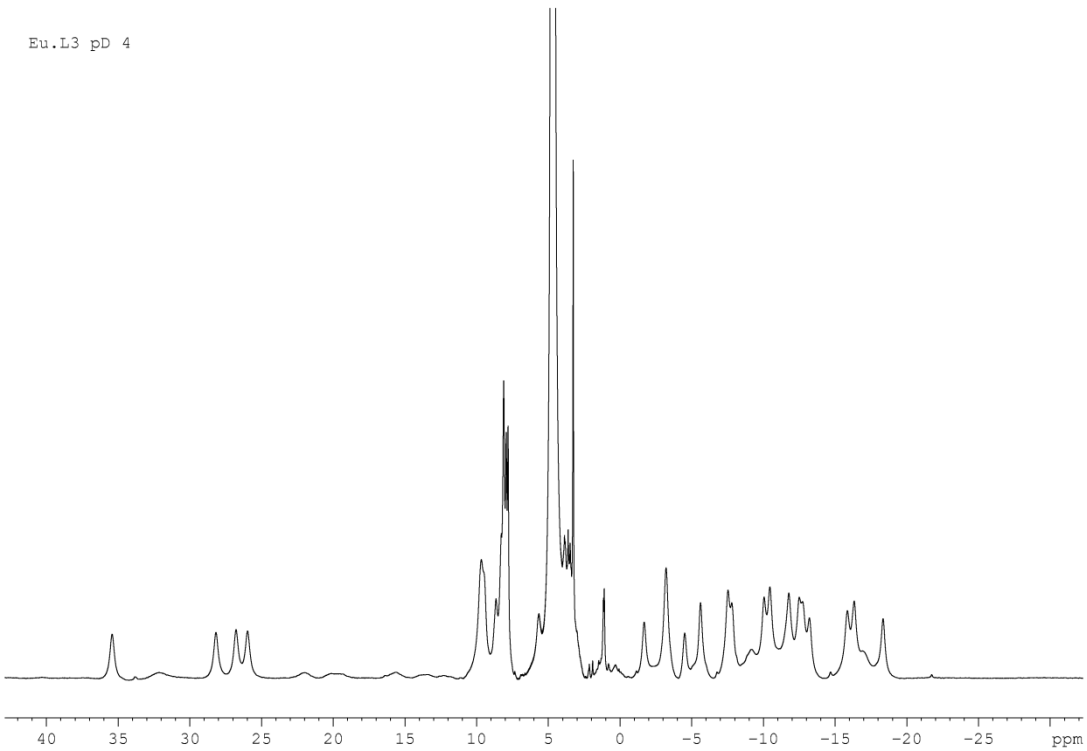

Figure S 10. ^{1}H-NMR of **Eu.L^3** in D_2O, pH 4, T = 298K.

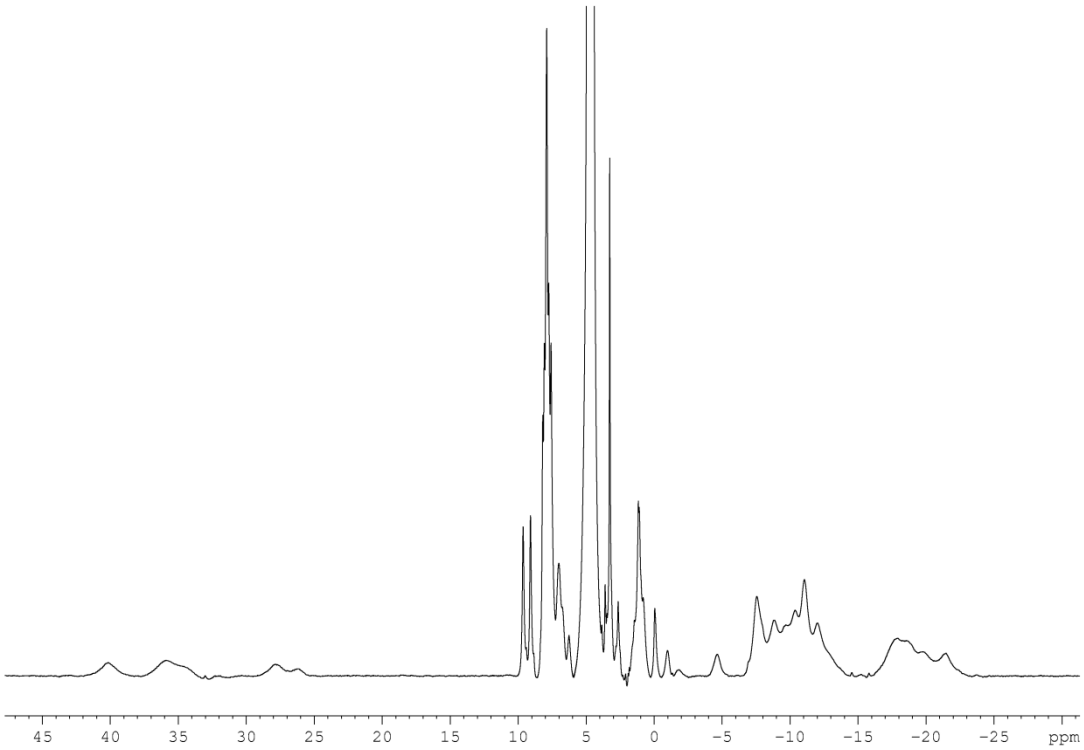

Figure S 11. ^{1}H-NMR of **Eu.L^3** in D_2O, pH 12, T = 298K.

NMR spectra of Yb.L^2

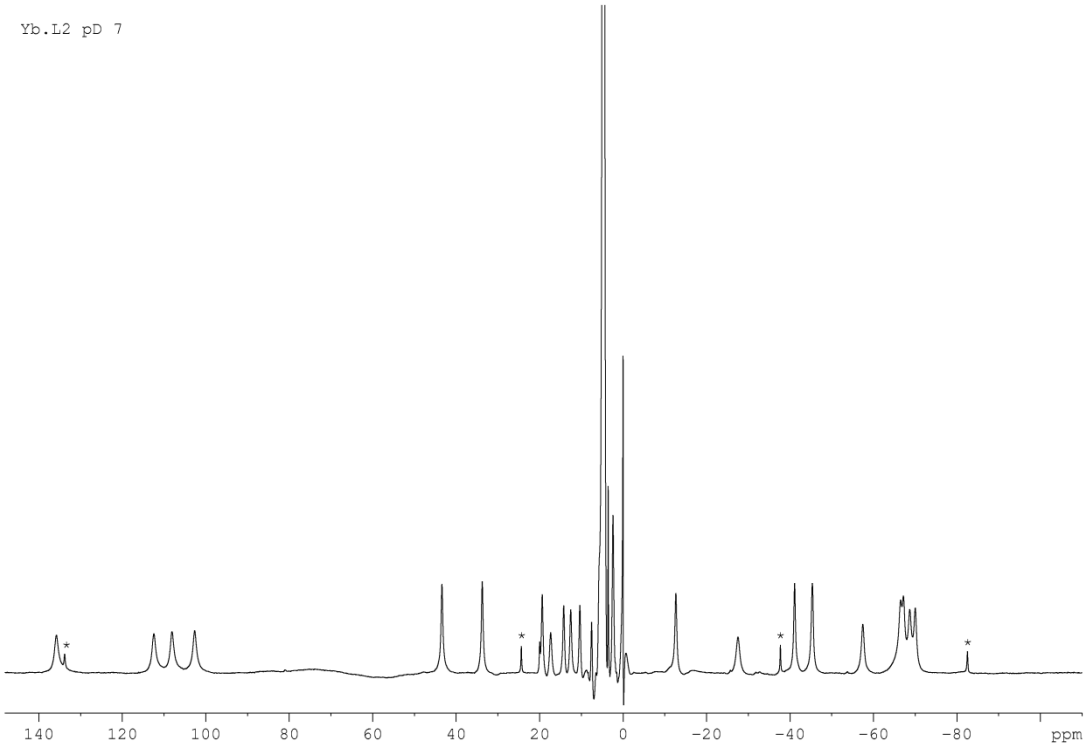

Figure S 12. ^{1}H-NMR of **Yb.L^2** in D_2O, pH 7, T = 298K. * indicates a small amount of [Yb(DOTA)]$^-$ present.

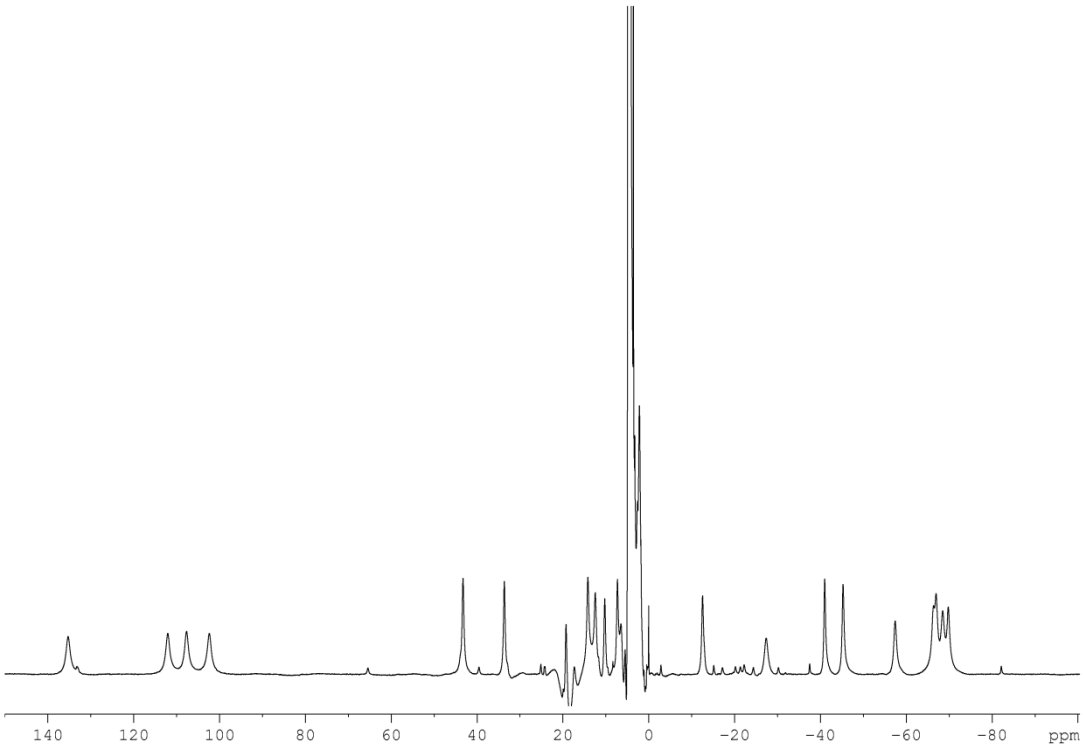

Figure S 13. ^{1}H-NMR of **Yb.L^2** in D_2O, pH 11, T = 298K.

NMR spectra of Yb.L^3 and [Yb.L^3]$^-$

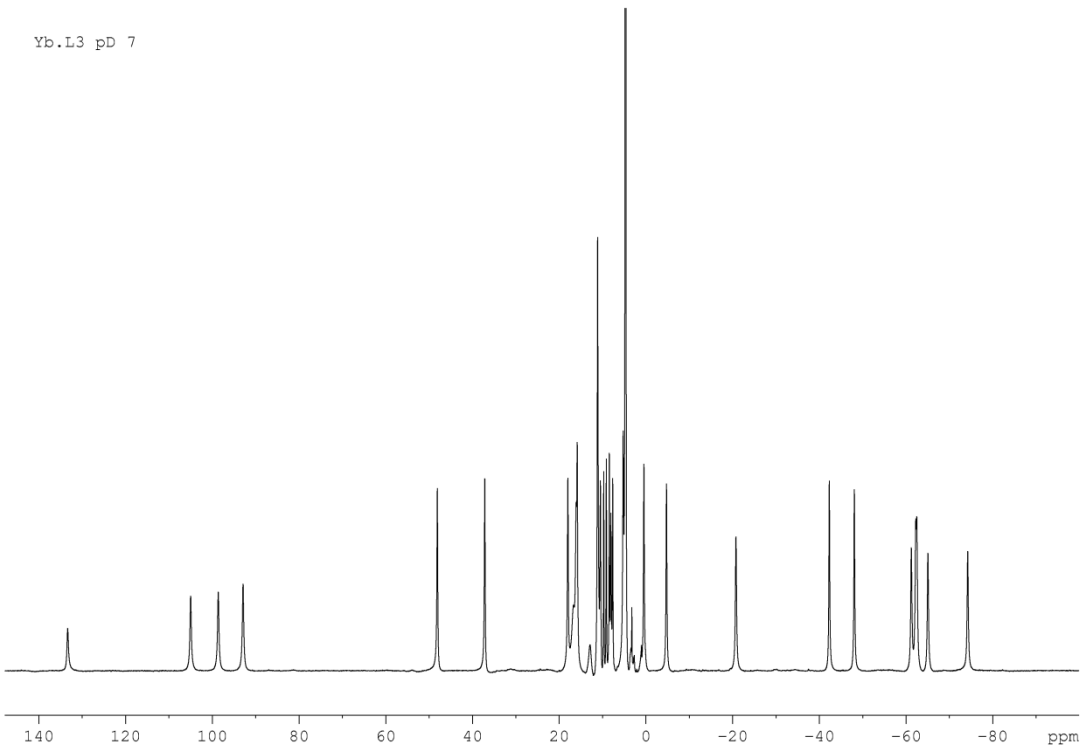

Figure S 14. ^{1}H-NMR of **Yb.L^3** in D_2O, pH 7, T = 298K.

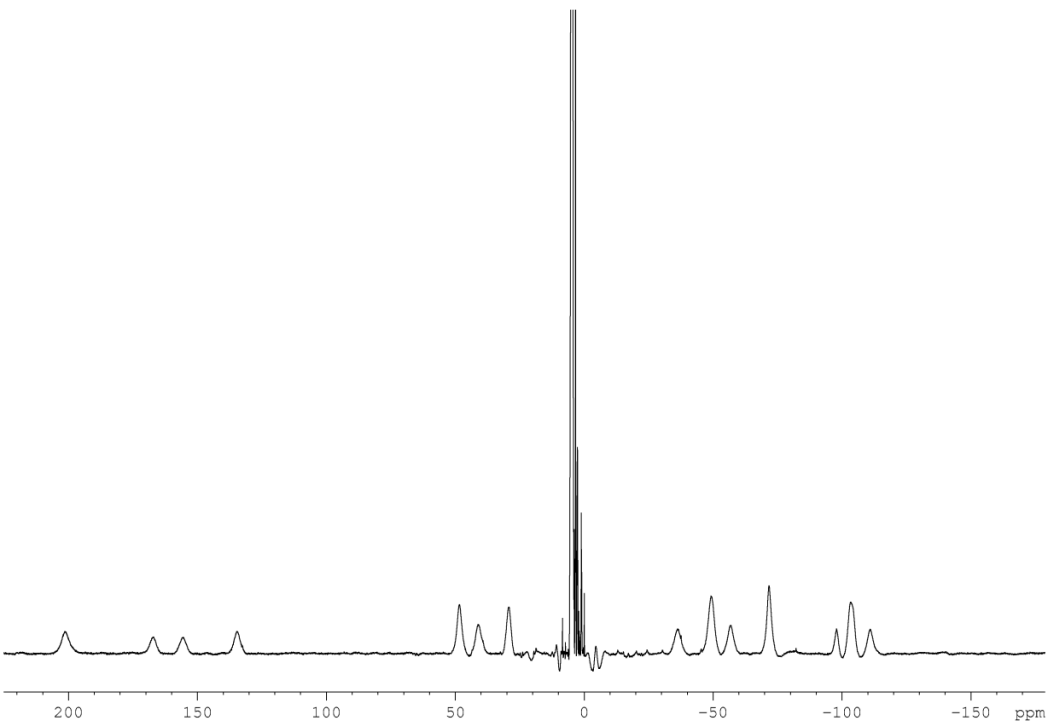

Figure S 15. ^{1}H-NMR of **Yb.L^3** in D_2O, pH 12, T = 298K.

Emission and UV-vis spectra

Comparison of emission spectra of Eu.L[1] at start and end of pH titration

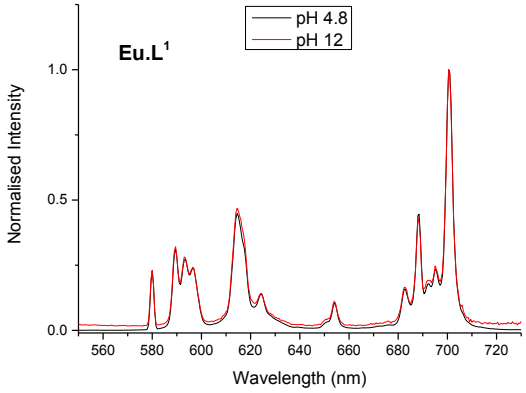

Figure S 16. Normalised emission spectra of **Eu.L[1]**.

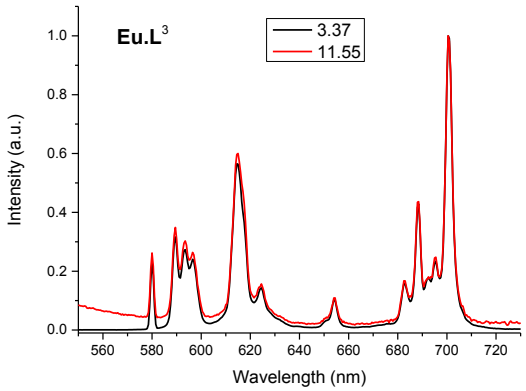

Figure S 17. Normalised emission spectra of **Eu.L[3]**.

pH dependent UV-Vis absorption and emission spectra of Ln(III) compounds

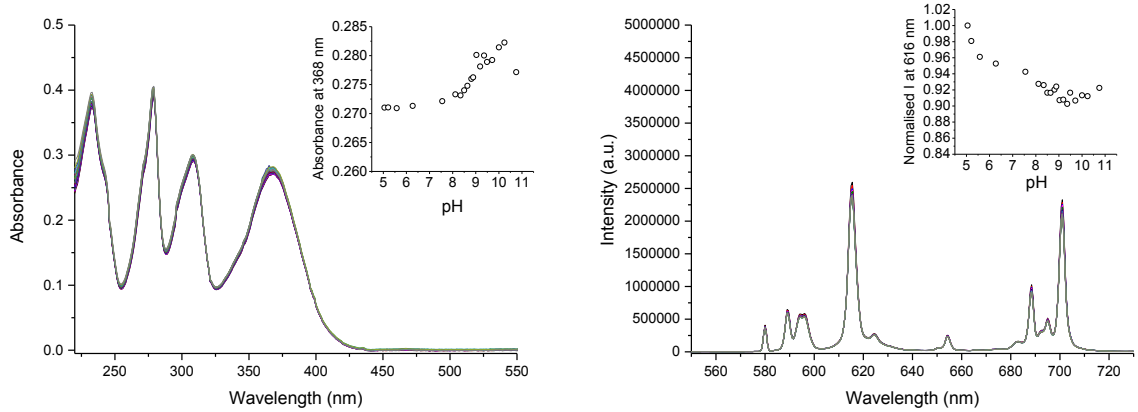

Figure S 18. pH dependence of the UV-Vis absorption and emission spectra of **Eu.L^2** (0.1M NaCl in H_2O, C = 1.8x10^{-5} M, T= 295 K, λ_{ex} = 367 nm).

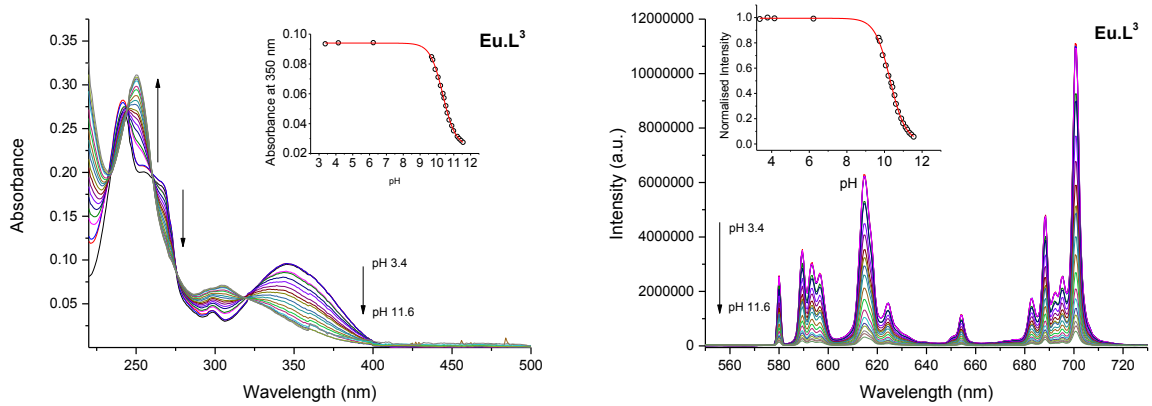

Figure S 19. pH dependence of the UV-Vis absorption and emission spectra of **Eu.L^3** (0.1M NaCl in H_2O, C = 4.8x10^{-6} M, T= 295 K, λ_{ex} = 347 nm).

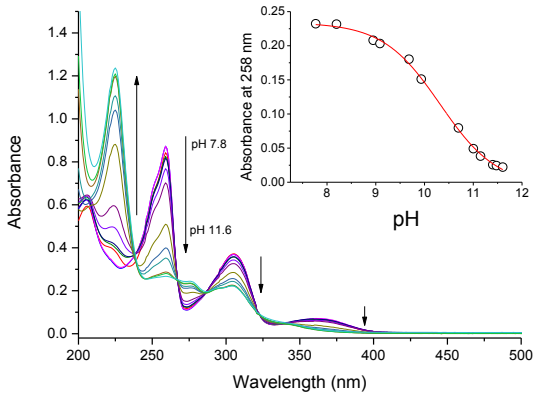

Figure S 20. pH dependence of the UV-Vis absorption of **Yb.L**[1] (0.1M NaCl in H_2O, C = 1.4x10^{-5} M, T= 295 K) pka 10.3.

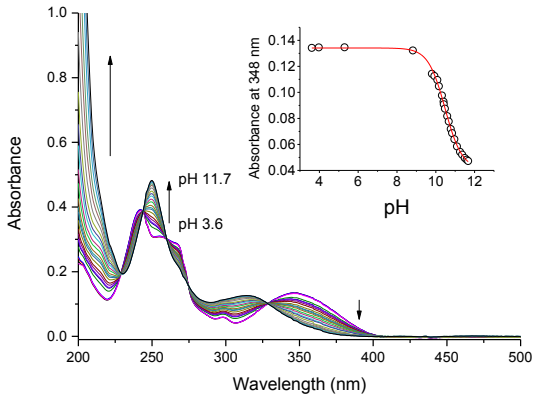

Figure S 21. pH dependence of the UV-Vis absorption of **Yb.L**[3] (0.1M NaCl in H_2O, C = 6.8x10^{-6} M, T= 295 K) in water. pka 10.5.

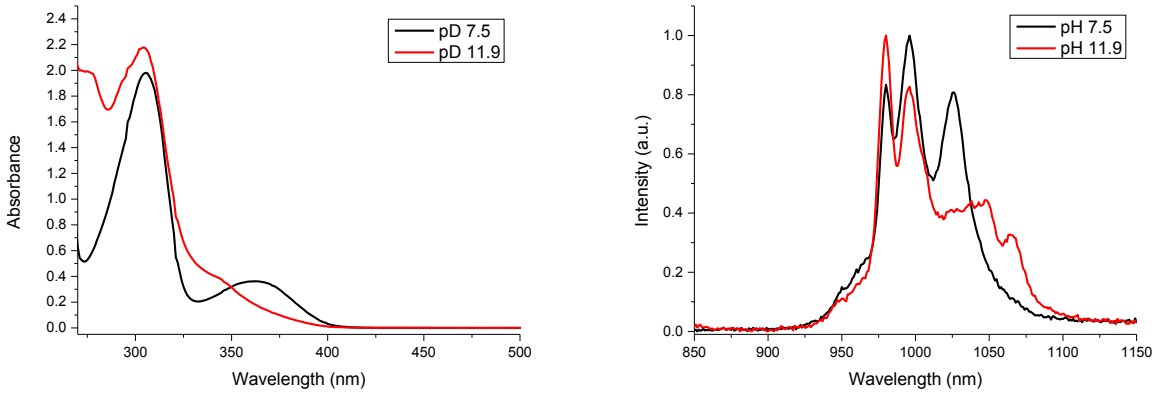

Figure S 22. pH dependence of the UV-Vis absorption and emission spectrum of **Yb.L**[1] (in D_2O, T= 295 K, λ_{ex} = 320 nm).

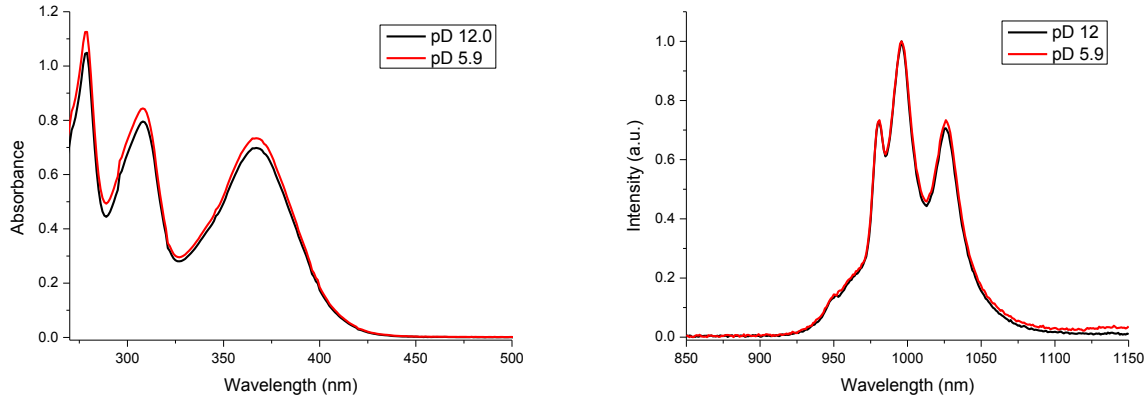

Figure S 23. pH dependence of the UV-Vis absorption and emission spectrum of **Yb.L^2** (in D_2O, T= 295 K, λ_{ex} = 370 nm).

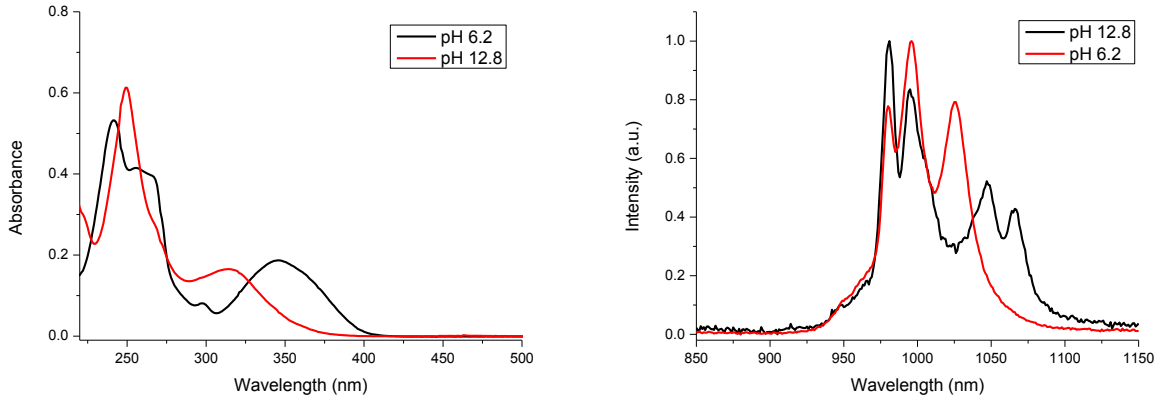

Figure S 24. pH dependence of the UV-Vis absorption and emission spectrum of **Yb.L^3** (in D_2O, T= 295 K, λ_{ex} = 320 nm).

Lifetime emission decay curves of lanthanide complexes

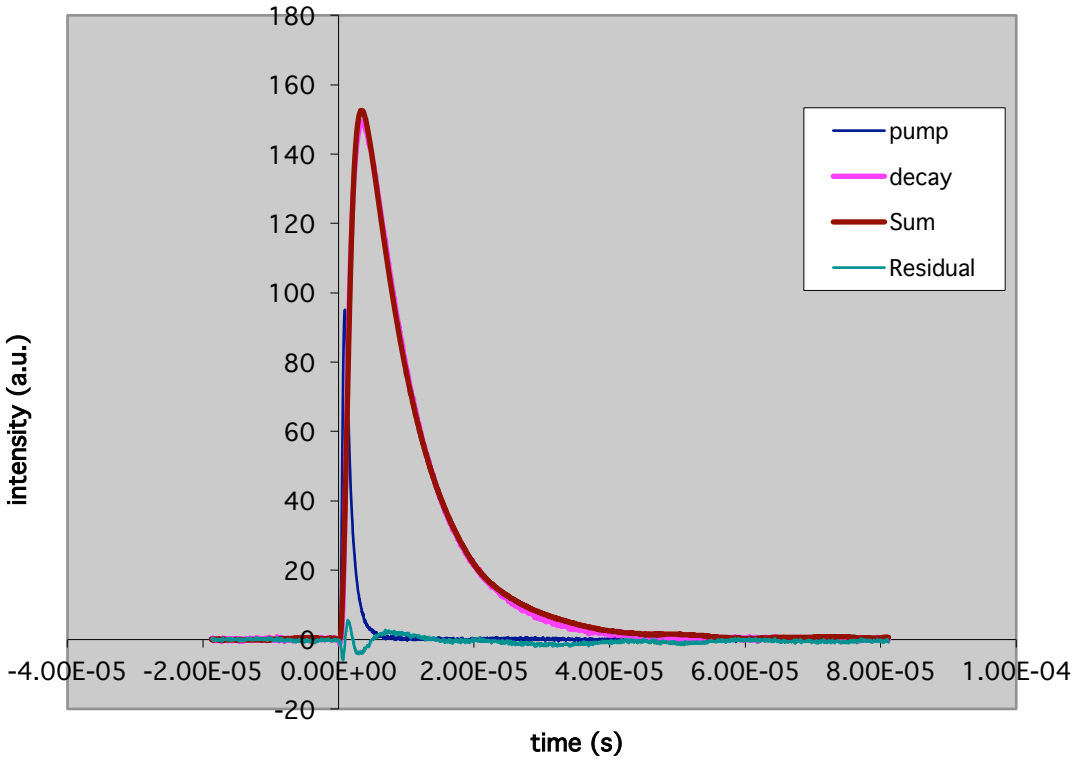

Figure S 25. Emission decay profile of **Yb.L**[1] in D_2O, pH 7.1, T= 295 K, λ_{ex} = 337 nm. "Pump": detector response, "decay": experimental emission decay profile, "sum" fitted decay profile, "residual": residuals difference between "sum" and "decay".

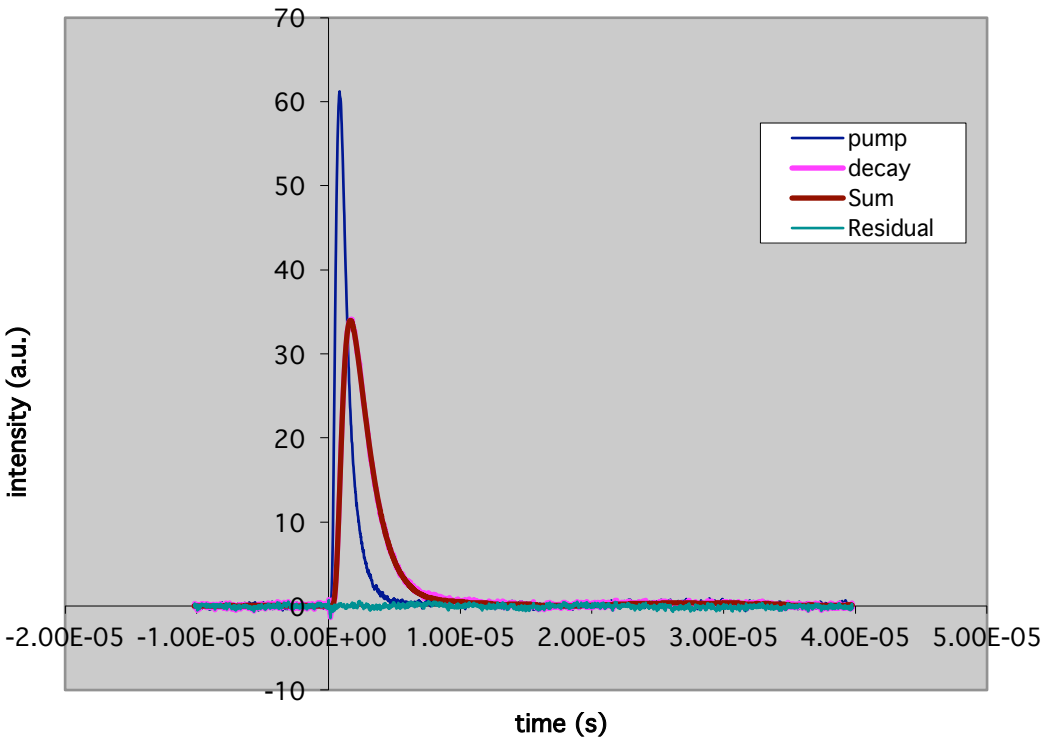

Figure S 26. Emission decay profile of **Yb.L**[1] in H_2O, pH 6.40, T= 295 K, λ_{ex} = 337 nm. "Pump": detector response, "decay": experimental emission decay profile, "sum" fitted decay profile, "residual": residuals difference between "sum" and "decay".

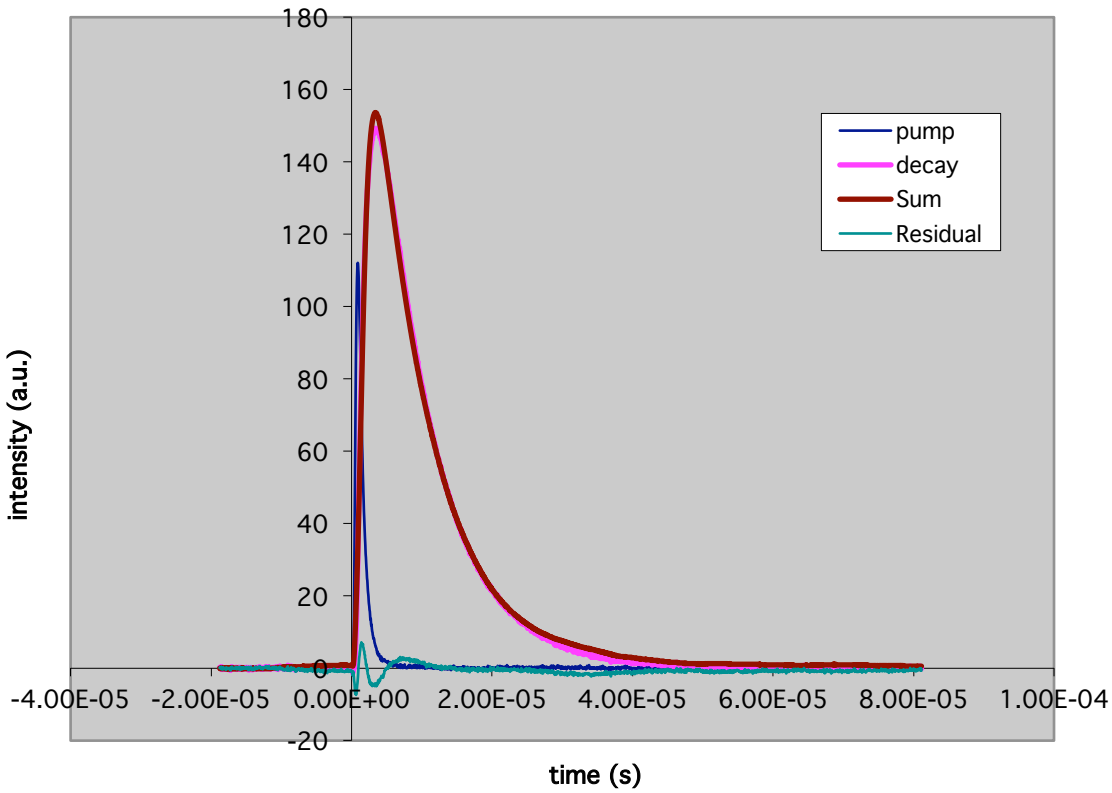

Figure S 27. Emission decay profile of [**Yb.L**^{1}]$^-$ in D_2O, pH 11.5, T= 295 K, λ_{ex} = 337 nm. "Pump": detector response, "decay": experimental emission decay profile, "sum" fitted decay profile, "residual": residuals difference between "sum" and "decay".

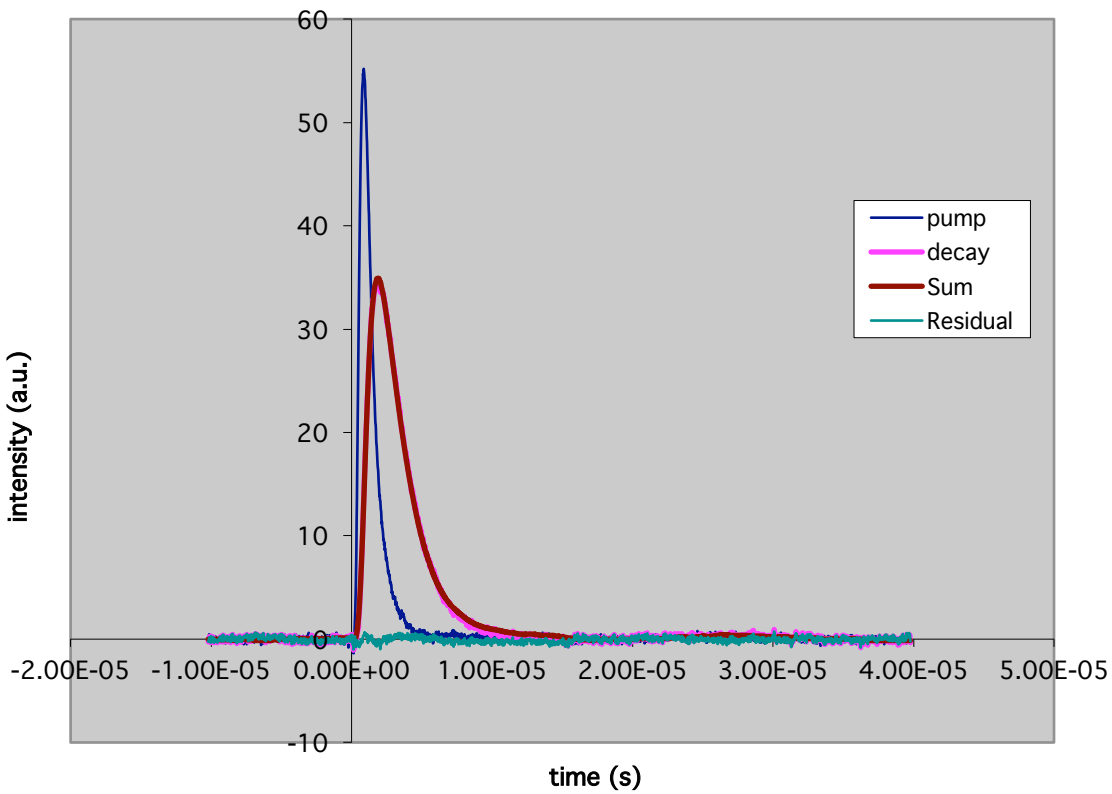

Figure S 28. Emission decay profile of [**Yb.L**^{1}]$^-$ in H_2O, pH 11.48, T= 295 K, λ_{ex} = 337 nm. "Pump": detector response, "decay": experimental emission decay profile, "sum" fitted decay profile, "residual": residuals difference between "sum"

and “decay”.

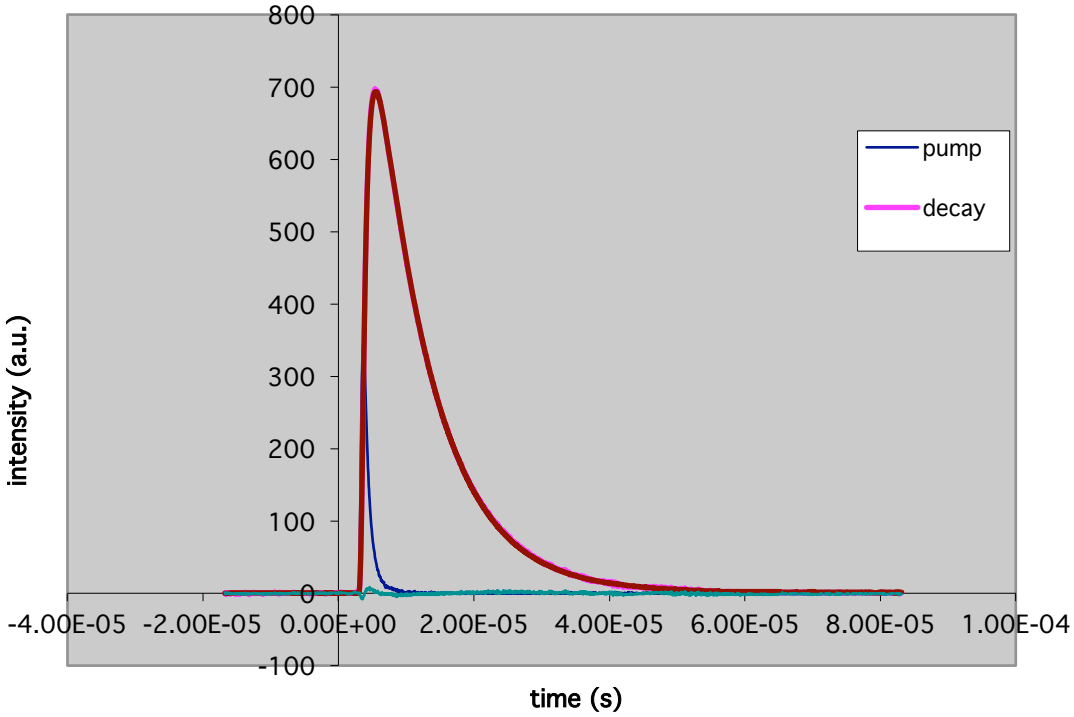

Figure S 29. Emission decay profile of **Yb.L**^{2} in D_2O, pH 5.4, T= 295 K, λ_{ex} = 337 nm. “Pump”: detector response, “decay”: experimental emission decay profile, “sum” fitted decay profile, “residual”: residuals difference between “sum” and “decay”.

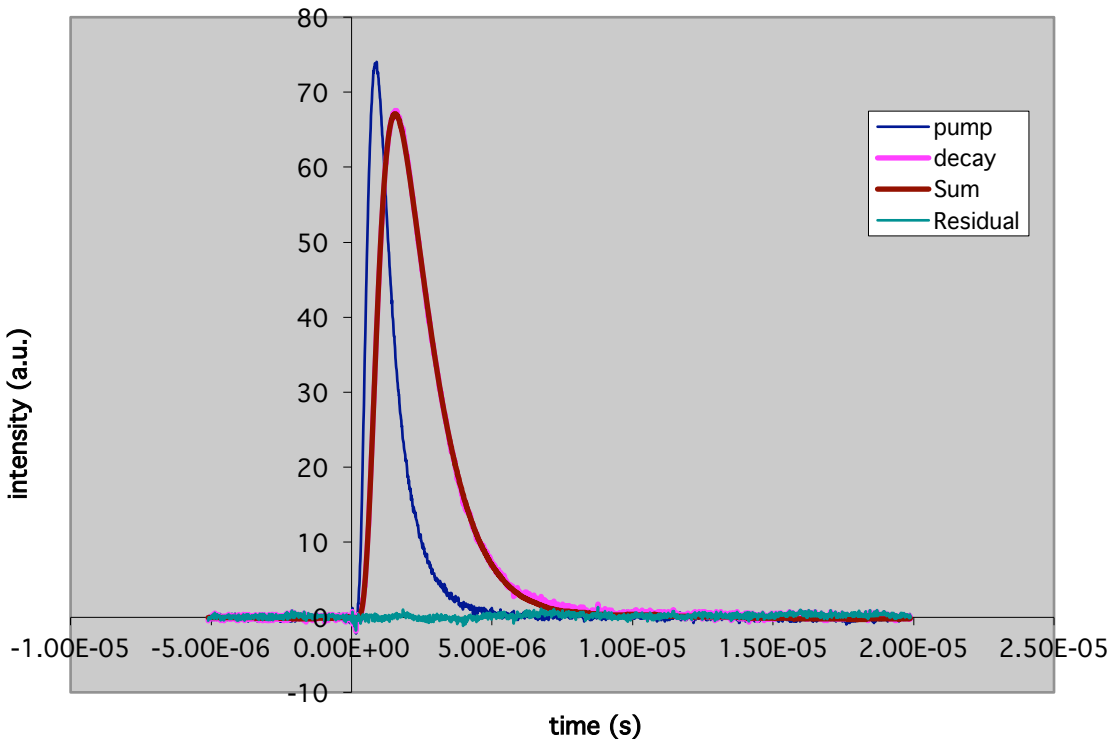

Figure S 30. Emission decay profile of **Yb.L**^{2} in H_2O, pH 4.7, T= 295 K, λ_{ex} = 337 nm. “Pump”: detector response, “decay”: experimental emission decay profile, “sum” fitted decay profile, “residual”: residuals difference between “sum” and

"decay".

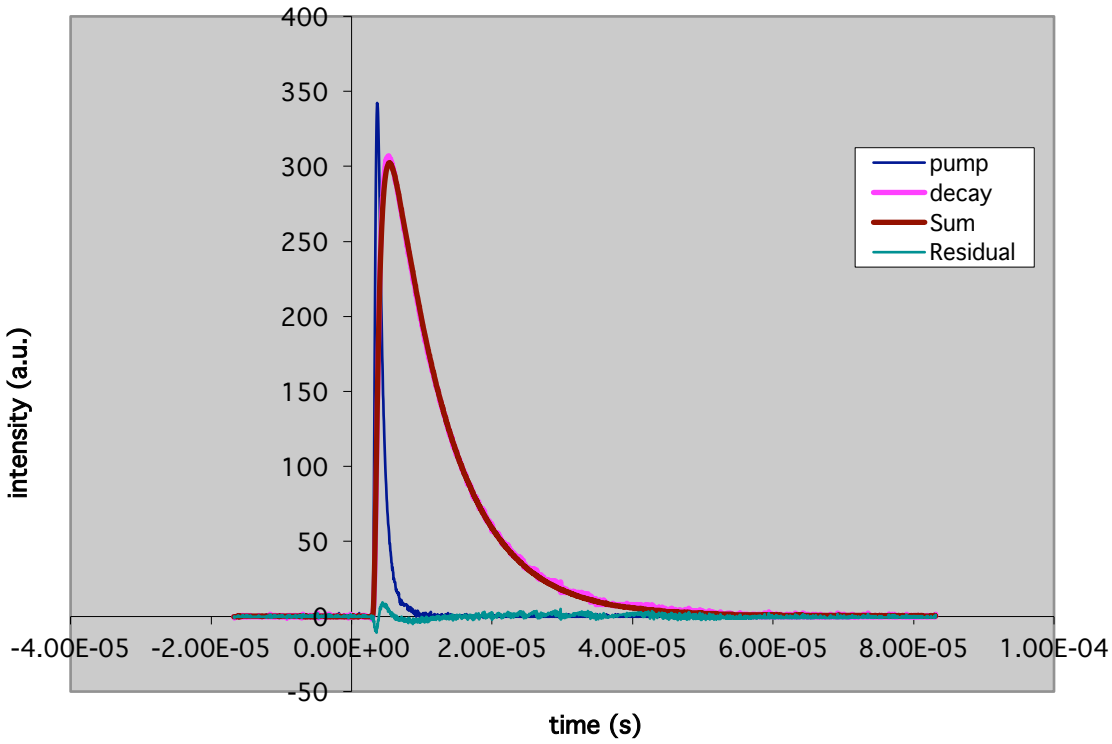

Figure S 31. Emission decay profile of [**Yb.L**^{2}]$^-$ in D_2O, pH 11.5, T= 295 K, λ_{ex} = 337 nm. "Pump": detector response, "decay": experimental emission decay profile, "sum" fitted decay profile, "residual": residuals difference between "sum" and "decay".

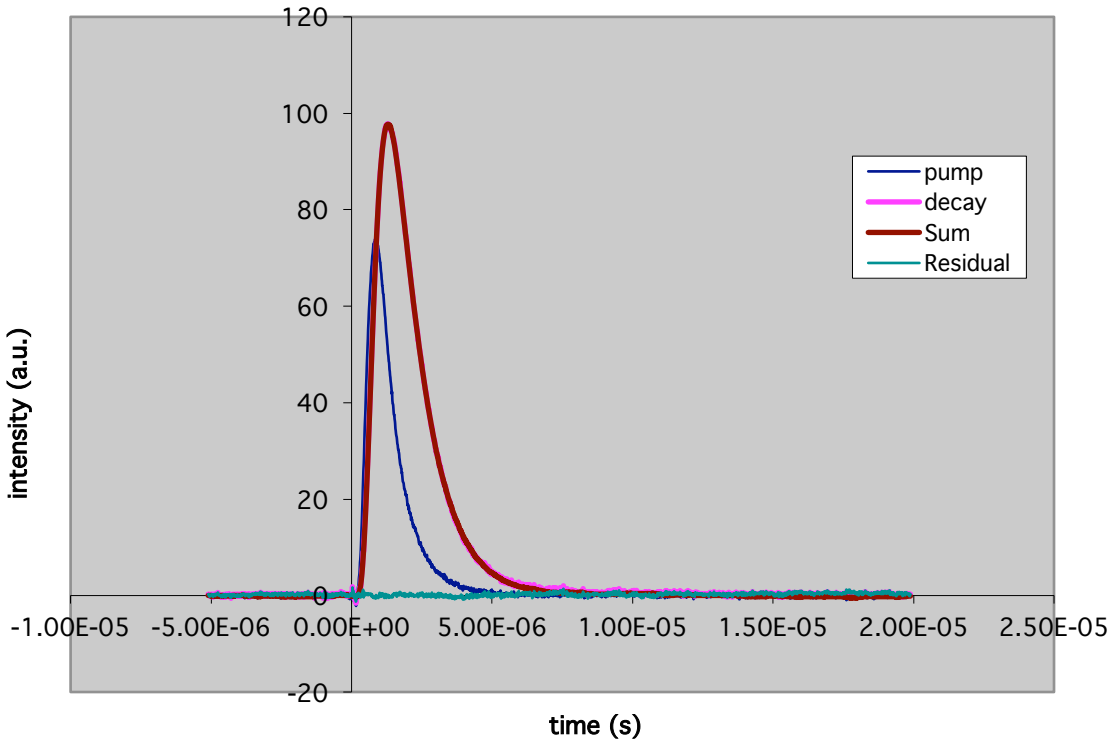

Figure S 32. Emission decay profile of [**Yb.L**^{2}]$^-$ in H_2O, pH 11.1, T= 295 K, λ_{ex} = 337 nm. "Pump": detector response, "decay": experimental emission decay profile, "sum" fitted decay profile, "residual": residuals difference between "sum" and "decay".

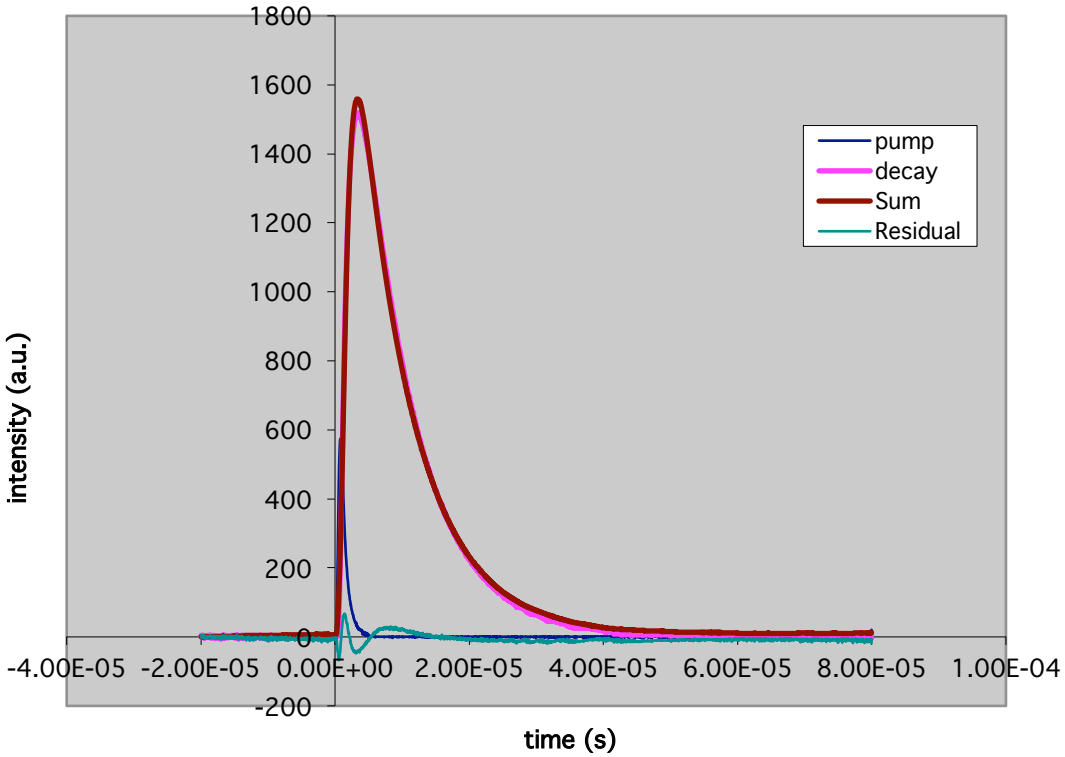

Figure S 33. Emission decay profile of **Yb.L**[3] in D_2O, pH 7.8, T= 295 K, λ_{ex} = 337 nm. "Pump": detector response, "decay": experimental emission decay profile, "sum" fitted decay profile, "residual": residuals difference between "sum" and "decay".

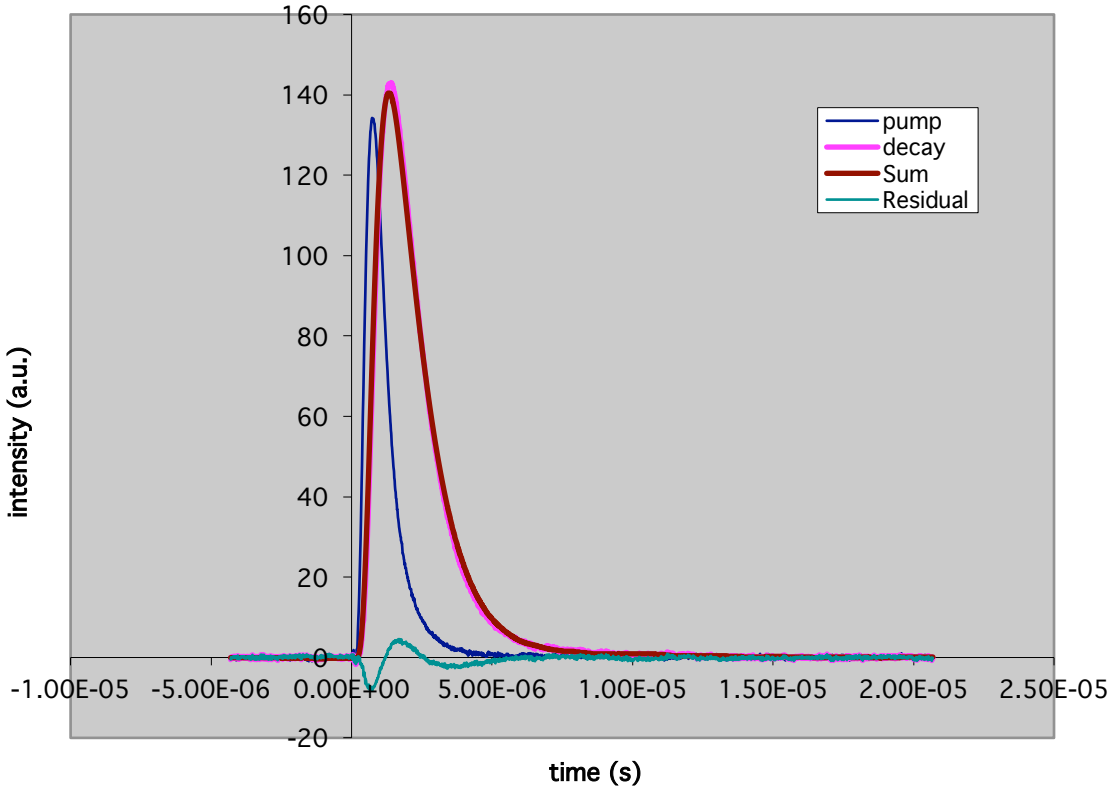

Figure S 34. Emission decay profile of **Yb.L**[3] in H_2O, pH 7.2, T= 295 K, λ_{ex} = 337 nm. "Pump": detector response, "decay": experimental emission decay profile, "sum" fitted decay profile, "residual": residuals difference between "sum" and "decay".

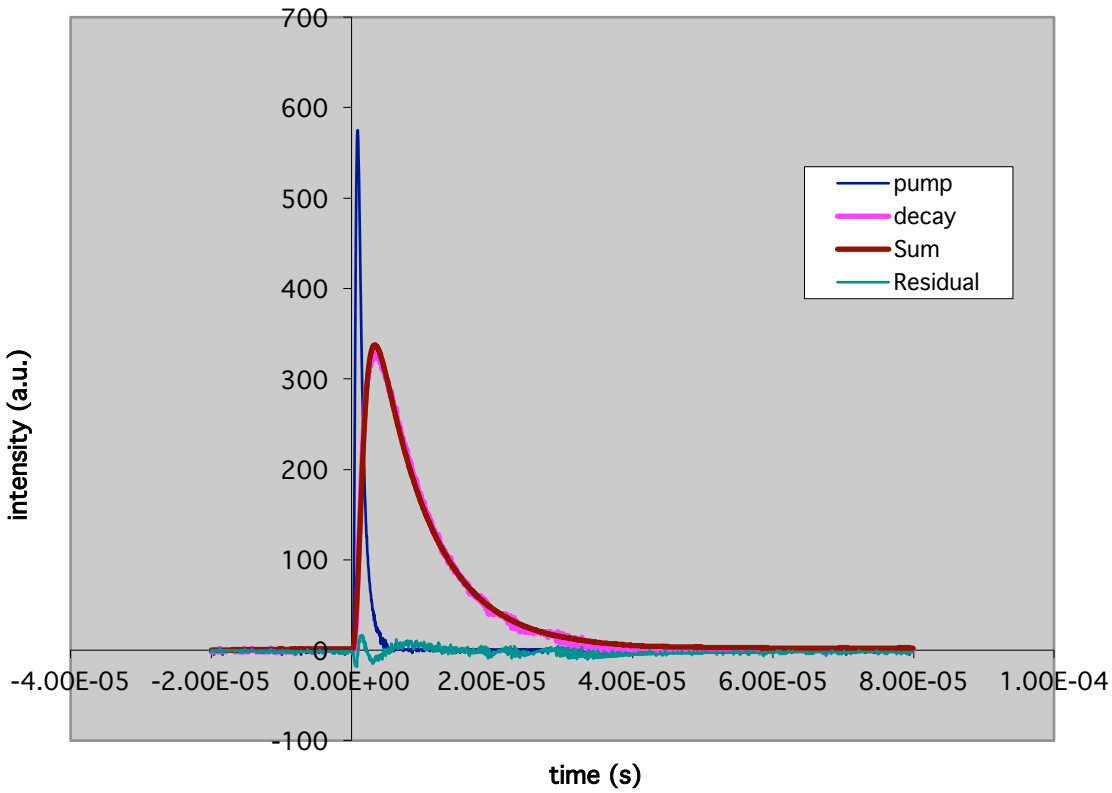

Figure S 35. Emission decay profile of [**Yb.L**^{3}]$^-$ in D_2O, pH 12.3, T= 295 K, λ_{ex} = 337 nm. "Pump": detector response, "decay": experimental emission decay profile, "sum" fitted decay profile, "residual": residuals difference between "sum" and "decay".

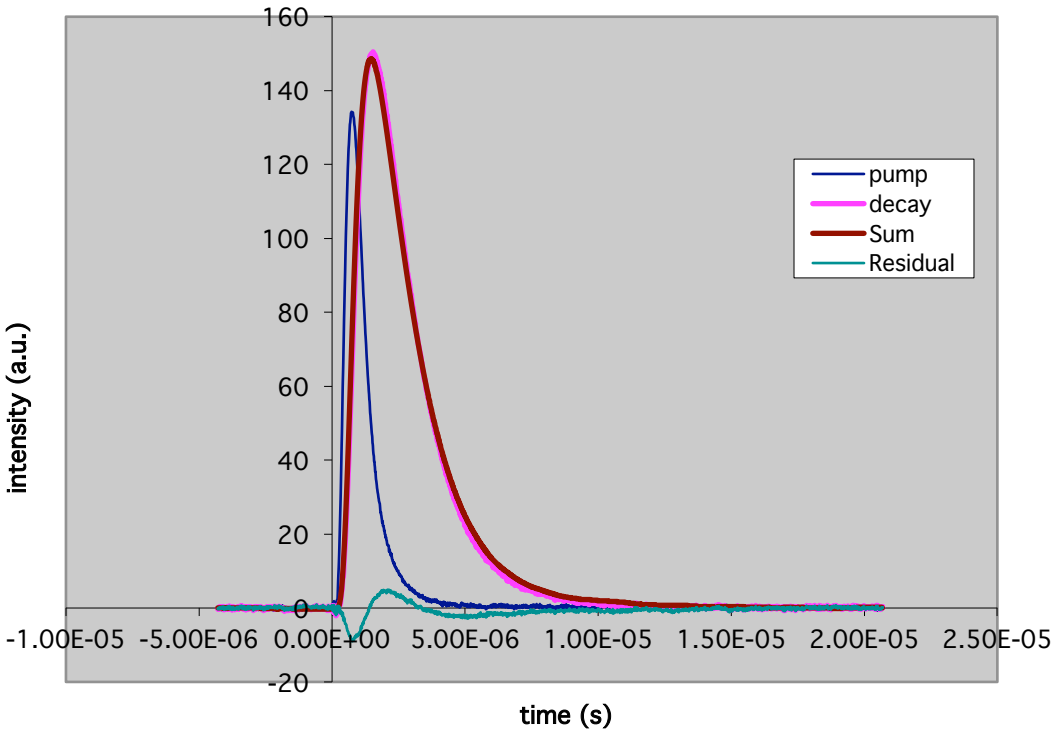

Figure S 36. Emission decay profile of [**Yb.L**^{3}]$^-$ in H_2O, pH 11.7, T= 295 K, λ_{ex} = 337 nm. "Pump": detector response, "decay": experimental emission decay profile, "sum" fitted decay profile, "residual": residuals difference between "sum" and "decay".

X-ray Crystallography

Single crystal X-ray diffraction data were obtained for compounds **S3**. A typical crystal was mounted using the oil drop technique, in perfluoropolyether oil at 150(2) K using a Cryostream N_2 open-flow cooling device.[4] Diffraction data were collected using graphite monochromatic Mo-K_α radiation (λ = 0.71073 Å) on a Nonius Kappa CCD diffractometer. For all data collections, series of ω-scans were performed in such a way as to collect a complete data set to a maximum resolution of 0.77 Å. Data reduction including unit cell refinement and inter-frame scaling was carried out using DENZO-SMN/SCALEPACK.[5] Intensity data were processed and corrected for absorption effects by the multi-scan method, based on repeat measurements of identical and Laue equivalent reflections. Structure solution was carried out with direct methods using the program SIR92[6] within the CRYSTALS software suite.[7] Coordinates and anisotropic displacement parameters of all non-hydrogen atoms were refined freely. Hydrogen atoms were generally visible in the difference map and refined with soft restraints prior to inclusion in the final refinement using a riding model.[8] A summary of the X-ray crystallographic data is provided below (Table **S1.**) and ORTEP depictions of the single crystal X-ray structures follow (Fig **S 37.**) Crystallographic data (excluding structure factors) for all the structures have been deposited with the Cambridge Crystallographic Data Centre (CCDC 1040048).

Single crystals of compound **S3** suitable for X-ray diffraction studies were grown slow evaporation of ethyl acetate:hexane 1:1. The crystals and refinement data are shown in table **S1**.

Compound	**S3**
Empirical formula	$C_{16}H_{14}ClNO$
Formula weight	271.74
Temperature/K	150
Crystal system	Orthorhombic
Space group	P 21 21 21
Unit cell dimensions	
a/Å	6.9474(10)
b/Å	13.2522(2)
c/Å	14.1927(2)
α/°	90
β/°	90
γ/°	90
Volume/Å^3	1306.70 (3)

Z	4
Calculated density/Mg m^{-3}	1.381
Absorption coefficient/ mm^{-1}	0.282
F(000)	568
Crystal size/mm	0.18 x 0.28 x 0.28
ϑ range from data collection/°	$5.0 \leq \vartheta \leq 27.5$
Index ranges, *hkl*	$0 \leq h \leq 9$, $0 \leq k \leq 17$, $0 \leq l \leq 18$
Reflections collected/unique	24029/1714
Absorption correction	0.92, 0.95
Data/restraints/parameters	1714/0/173
Goodness-of-fit on F^2	1.0005
Final R indices [I > 2σ(I)]	0.0362
R indices (all data)	0.0461
Largest diff. peak and hole/e $Å^{-3}$	-0.32, 0.28
CCDC number	1040048

Table S1. Crystal data and structure refinement parameters.

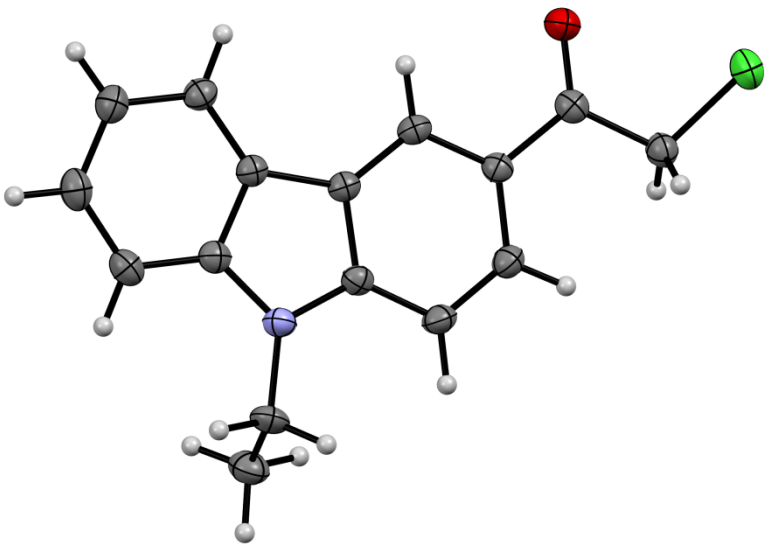

Figure S 37. ORTEP representation of the X-ray crystal structure of **S3** with thermal ellipsoids at 50% probability.

References

[1] A. Krężel and W. Bal, *J. Inorg. Biochem.*, **2004**, *98*, 161-166.

[2] a) A. S. Chauvin, F. Gumy, D. Imbert and J. C. G. Bünzli, *Spectrosc. Lett.*, **2004**, *37*, 517-532; b) *Spectrosc. Lett.*, **2007**, *40*, 193-193.

[3] N. P. Buu-HoÏ and R. Royer, *The Journal of Organic Chemistry*, **1950**, *15*, 123-130.

[4] J. Cosier and A. M. Glazer, *J. Appl. Crystallogr.*, **1986**, *19*, 105-107.

[5] Z. Otwinowski and W. Minor, *Macromol Crystallography Part A* **1997**, 307-326.

[6] A. Altomare, G. Cascarano, C. Giacovazzo and A. Guagliardi, *J. Appl. Crystallogr.*, **1994**, *27*, 1045-1050.

[7] D. Watkin, R. Cooper and C. K. Prout, *Zeitschrift für Kristallographie*, **2002**, *217*, 429.

[8] R. I. Cooper, A. L. Thompson and D. J. Watkin, *J. Appl. Crystallogr.*, **2010**, *43*, 1100-1107.